PERGAMON

International Journal of Heat and Mass Transfer 46 (2003) 749–754

International Journal of HEAT and MASS TRANSFER

www.elsevier.com/locate/ijhmt

Numerical study of stratified oil–water two-phase turbulent flow in a horizontal tube

Hui Gao, Han-Yang Gu, Lie-Jin Guo *

State Key Laboratory of Multiphase Flow in Power Engineering, Xi'an Jiaotong University, Xi'an, Shaanxi Province 710049, China

Received 14 June 2002

Abstract

Stratified oil–water two-phase turbulent flow in a horizontal tube is numerically simulated using a volume of fluid model. A single momentum equation is solved throughout the domain. The RNG k–ε model combined with a near-wall low-*Re* turbulence model is applied to each phase, and a continuum surface force approximation is adopted for the calculation of surface tension. The simulation is performed in a time-dependent way and the final solution which corresponds to steady-state flow is analyzed. Results of pressure loss, slip ratio, local phase fraction profile and the axial velocity profile are verified by experimental data in literature. Based on the numerical results of extensive calculations, the flow field characteristics are explored and correlations for pressure loss and hold-up are presented.

Keywords: Stratified two-phase flow; Turbulence; Numerical simulation; VOF model

1. Introduction

Stratified two-phase pipe flow is frequently encountered in the petroleum and chemical processing industries. The prediction of pressure drop and holdup in stratified two-phase pipe flow has been of considerable research interest since the 1930s. Early investigators developed many empirical correlations based on different flow conditions to analyze the flow characteristics, namely, pressure drop and in situ holdup [1,2]. However, the predictive capabilities are generally restricted to the flow conditions on which they are based [3–5].

Mechanistic models for stratified pipe flows [6–9] have been developed based on the interpretation of the dominant physical mechanisms of the process. For the lack of knowledge about the distribution of wall shear in stratified pipe flows, expediential recourse is often made to relations established in single-phase pipe flow, with a resulting loss in calculation accuracy. Computational fluid dynamics (CFD) techniques have been applied to the calculation of the stratified pipe flows. One of the early CFD models of turbulent stratified flow in a horizontal pipe was presented by Shoham and Taitel [10]. A two-dimensional axial momentum equation and a zero-equation turbulence model were used to calculate the liquid region flow field, while the gas region was treated as a bulk flow, with additional shear generated by a wavy interface modeled by an empirical friction factor. Solutions for turbulent liquid flows were obtained in horizontal and slightly inclined pipes of 25.4 mm diameter. Issa [11] numerically simulated the stratified gas–liquid pipe flow, using standard k–ε turbulence model with wall functions for each phase. Newton and Behnia [12] obtained more satisfactory solutions for stratified pipe flow by employing a low Reynolds number turbulent model instead of wall functions.

Stratified oil–water two-phase pipe flow is commonly found in oil production and transport. Elseth et al. [13] simulates the turbulent stratified oil–water pipe flow using a volume of fluid (VOF) model. However, their numerical results are not acceptable when compared with their measured data. In the present paper, a modified VOF model is applied to compute turbulent smooth-stratified oil–water two-phase flow in a horizontal pipe, and the continuum surface force (CSF) model proposed by Brackbill et al. [14] is used to including the effect of

* Corresponding author. Tel./fax: +86-29-2668769.
E-mail address: lj-guo@xjtu.edu.cn (L.-J. Guo).

0017-9310/03/$ - see front matter
PII: S0017-9310(02)00321-6

Nomenclature

A	flow cross-sectional area, m^2
A_μ, A_1, A_c	coefficient in Eqs. (13) and (14)
C_μ, C_1, C_2	coefficient in low-Reynold k–ε model
f_μ, f_1, f_2	damping function in low-Re k–ε model
F	surface tension term, Nm^{-3}
g	acceleration of gravity, $m\,s^{-2}$
G	generation of turbulence kinetic energy, $m\,s^{-3}$
k	turbulence kinetic energy, $m^2\,s^{-2}$
n	unit normal vector to a surface, m
p	pressure, Pa
Re	Reynold number
S	slip ratio
t	time, s
u	velocity in the x direction, $m\,s^{-1}$
U	velocity vector, $m\,s^{-1}$
v	velocity in the y direction, $m\,s^{-1}$
x, y, z	Descartes coordinates, m
X	Martinelli parameter

Greek symbols

α	holdup of phases
β	volume fraction of phases
υ	kinematic viscosity, $m^2\,s^{-1}$
ε	turbulence dissipation, $m^2\,s^{-3}$
ϕ	ratio of superficial velocity
μ	dynamic viscosity, $kg\,m^{-1}\,s^{-1}$
θ	local volume fraction of phases
η	normal distance vector from the wall at the cell centers, m
κ	curvature, m^{-1}
ρ	density, $kg\,m^{-3}$
σ	surface tension coefficient in Eq. (6), Nm^{-1}
σ_k, σ_ε	coefficient in low-Reynold k–ε model

Subscripts

o	oil phase
s	surface
so	superficial for oil phase
sw	superficial for water phase
t	turbulence
w	water phase

surface tension. Turbulence is simulated here by a two-layer turbulence model. The simulation is performed in a time-dependent way so that the numerical stabilization could be achieved. Then the final solution which corresponds to steady-state flow can be analyzed.

2. Modelling method

2.1. Governing equations

Consider the stratified two-phase flow in a horizontal pipe as shown schematically in Fig. 1. With the VOF model used, the fields for all variables (pressure, velocity, etc.) are defined as volume averaged. It is thus necessary to know the local volume fraction of each phase in the entire computation domain. The local volume fraction of the oil, θ_o, is given by the following continuity equation:

$$\frac{\partial \theta_o}{\partial t} + \nabla \cdot (\theta_o U_o) = 0 \tag{1}$$

The local volume fraction of water, θ_w, should be

$$\theta_w = 1 - \theta_o \tag{2}$$

Single momentum equation shown below is solved throughout the domain. The momentum equation is dependent on the volume fractions of two phases as

$$\frac{\partial(\rho U)}{\partial t} + \nabla \cdot (\rho U \times U) = -\nabla p + \rho g + \nabla \cdot [\mu(\nabla U + \nabla U^T)] + F_s \tag{3}$$

ρ and μ being given by

$$\rho = \theta_w \rho_w + \theta_o \rho_o \tag{4}$$

$$\mu = \theta_w \mu_w + \theta_o \mu_o \tag{5}$$

The last term in Eq. (3), F_s, is the external force per unit volume and can be modeled using the CSF model developed by Brackbill et al. [14]. An interface is interpolated as a transient region with a finite thickness. Thus the surface tension localized in the region is converted into a volume force with the help of a Dirac delta function concentrated in the surface as

$$F_s = 2\sigma\kappa\theta_o \nabla\theta_o \tag{6}$$

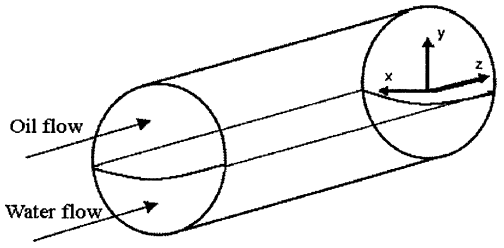

Fig. 1. Schematic representation of pipe flow.

The curvature, κ, is given by

$$\kappa = (\nabla \cdot \hat{\boldsymbol{n}}) = \frac{1}{|n|}\left[\left(\frac{n}{|n|}\cdot\nabla\right)|n| - (\nabla \cdot n)\right] \tag{7}$$

Here, n is a unit normal vector to a surface, defined in term of the oil phase volume fraction, θ_o, as

$$n = \nabla\theta_o \tag{8}$$

2.2. Turbulence model adapted

The turbulent viscosity is calculated here by using a two-layer turbulence model. The whole computation domain is divided into a viscosity-affected region and a fully turbulent region determined by a wall-distance-based turbulent Reynolds number, Re_η, defined as

$$Re_\eta = \frac{\rho\sqrt{k}\eta}{\mu} \tag{9}$$

where η is the normal distance from the wall at the cell centers. In the fully turbulent region ($Re_\eta > 200$), a RNG k–ε model is employed, while in the viscosity-affected near-wall region ($Re_\eta < 200$), a low Reynolds number k–ε model is employed. The RNG k–ε model is derived using a rigorous statistical technique, which has an additional term in its ε equation that significantly improves the accuracy. In order to avoid using of wall functions, the low Reynolds number k–ε model given by Jones and Launder [15] is applied to model the flow near the pipes walls, where the viscous forces dominate. For the present system this is given by

$$\mu_t = f_\mu C_\mu \rho k^2/\varepsilon \tag{10}$$

$$\begin{aligned}\frac{\partial(\rho u k)}{\partial x} + \frac{\partial(\rho v k)}{\partial y} &= \frac{\partial}{\partial x}\left[\left(\mu + \frac{\mu_t}{\sigma_k}\right)\frac{\partial k}{\partial x}\right] \\ &\quad + \frac{\partial}{\partial y}\left[\left(\mu + \frac{\mu_t}{\sigma_k}\right)\frac{\partial k}{\partial y}\right] \\ &\quad + \mu_t G - \rho\varepsilon - 2\mu\left(\frac{\partial k^{1/2}}{\partial y}\right)^2\end{aligned} \tag{11}$$

$$\begin{aligned}\frac{\partial(\rho u \varepsilon)}{\partial x} + \frac{\partial(\rho v \varepsilon)}{\partial y} &= \frac{\partial}{\partial x}\left[\left(\mu + \frac{\mu_t}{\sigma_\varepsilon}\right)\frac{\partial \varepsilon}{\partial x}\right] + \frac{\varepsilon}{k}c_1 f_1 \mu_t G \\ &\quad - c_2 \rho f_2 \frac{\varepsilon^2}{k} + 2\frac{\mu\mu_t}{\rho}\left(\frac{\partial^2 u}{\partial y^2}\right)^2 \\ &\quad + \frac{\partial}{\partial y}\left[\left(\mu + \frac{\mu_t}{\sigma_\varepsilon}\right)\frac{\partial \varepsilon}{\partial y}\right]\end{aligned} \tag{12}$$

where $\sigma_k = 1.0$, $\sigma_\varepsilon = 1.3$, $C_\mu = 0.09$, $C_1 = 1.92$ and $C_2 = 1.3$. Closure of the model is thus achieved by prescribing the wall damping functions f_μ, f_1, and f_2.

The damping functions presented by Lam and Bremhorst [16] are adopted here

$$f_\mu = \left(1 - \exp(-A_\mu Re_\eta)\right)^2\left(1 + A_1/Re_\eta\right) \tag{13}$$

$$f_1 = 1 + (A_c/f_\mu)^3 \tag{14}$$

$$f_2 = 1 - \exp(-Re_\eta^2) \tag{15}$$

where $A_\mu = 0.0165$, $A_1 = 20.5$, $A_c = 0.05$.

2.3. Boundary conditions and interface treatment

The wall boundary conditions in both liquid regions are given by

$$w = k = \mu_t = 0 \tag{16}$$

$$\partial\varepsilon/\partial\eta = 0 \tag{17}$$

where η is the vector normal to the wall.

Convection and diffusion fluxes through the control volume faces must be computed and balanced with source terms within the control volume itself. In order to calculate convection and diffusion fluxes through the control volume faces, geometric reconstruction scheme is applied for the interface between fluids using a piecewise-linear approach. It assumes that the interface between two fluids is a linear slope within each cell, for calculating the advection of fluid through the cell faces. Firstly, the position of the linear interface relative to the center of each partially filled cell is calculated, based on information about the volume fraction and its derivatives in the cell. Then the advecting amount of fluid through each face is obtained using the computed linear interface representation and information about the normal and tangential velocity distribution on the face. Lastly, the volume fraction in each cell is given using the balance of fluxes calculated during the previous step. As it is illustrated in Fig. 2 the reconstruction of the interface is accomplished via the use of the geometric reconstruction scheme.

3. Results and analysis

The stratified oil–water two-phase turbulent flow in a 55.75 mm diameter, 8 m long horizontal tube is numerically simulated. The oil is a petroleum distillate with density of 790 kg/m^3 and dynamic viscosity of 1.6 cP at 25 °C. Input water volume fraction is in the range of 10–86%. The velocities of the two phases are specified to give a bulk velocity of 1.05 m/s and the maximum Reynolds numbers of oil and water reaching 55 000 and 110 000 respectively.

3.1. Pressure drop and slip ratio

Fig. 3(a) shows a comparison between the present predicted pressure drop and experimental data of Elseth et al.' [13]. The predicted result agrees well with the experimental data when the water volume fraction is in the range of 0.2–0.8. However, the great deviation appears

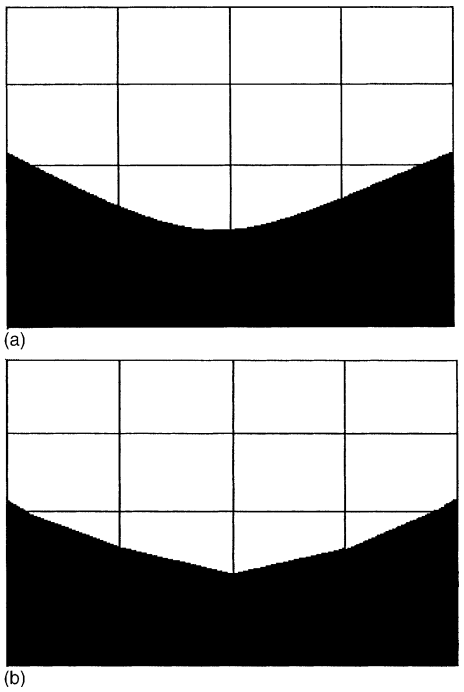

Fig. 2. Sketch of the interface calculation: (a) real shape of the interface, (b) shape calculated by VOF geometric reconstruction scheme.

when water fraction exceeds 0.8, the model under-predicts the experimental data with an error of 16% when the water volume fraction is 0.867. It may be due to the inherent limitation of present model that a single momentum equation is solved throughout the domain and the resulting velocity field is shared by the two liquid phases. Large velocity differences exist between the phases when the water fraction exceeds 0.8, and the velocity field computed near the interface is not reasonable enough. The slip ratio, S, is calculated as

$$S = \frac{u_o}{u_w} = \frac{A_w}{A_o}\frac{U_{so}}{U_{sw}} \tag{18}$$

where u_o and u_w are the mean velocities of the two phases, A_w and A_o are the flow area of water and oil, respectively. U_{so} is the superficial velocity of oil and U_{sw} is the superficial velocity of water.

Fig. 3(b) shows the comparison between predicted and experimental values of slip ratio. Generally, the predicted slip ratio closely matched, those given by Elseth et al.' [13]. It can be observed from Fig. 3(b) that the model slightly under-predicts the experimental data with an absolute average error of 6% when the water holdup is less than 0.5 and up-predicts the experimental data with an absolute average error of 8.2% when the water volume fraction is more than 0.5. The agreement in Fig. 3 appears very good when the model is used to

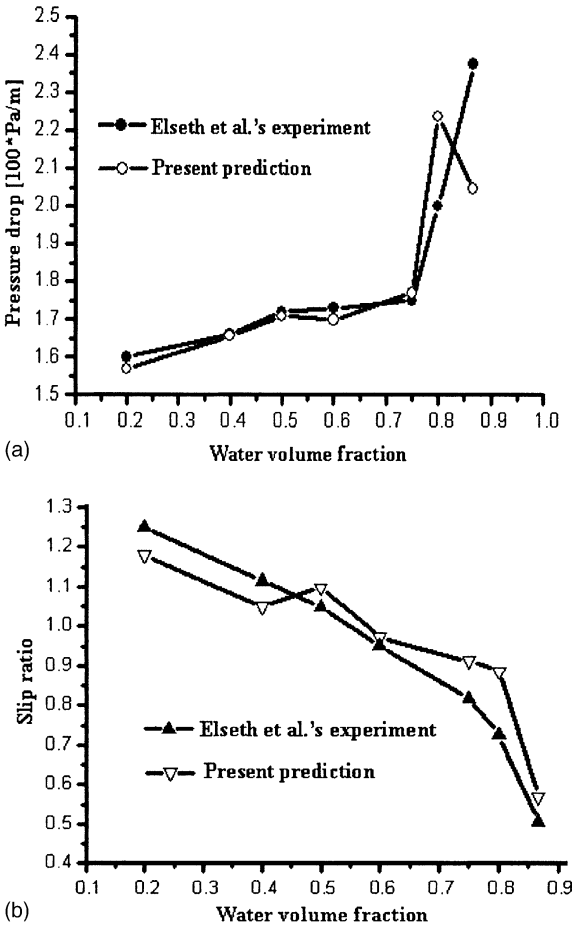

Fig. 3. Comparison between prediction and experiment values of pressure loss and slip ratio.

predict the pressure slip ratio at the water fraction of 0.2–0.8.

3.2. Local phase fraction

A series of calculated vertical local phase fraction profiles are compared with the experimental data of Elseth et al.' [13] in Fig. 4, the agreement is quite favorable. It can be observe, however, that the model slightly over-predicted the local water fraction on the upper part of the pipe at the water volume fraction of 75% and under-predicted at the water volume fraction of 25%. It may be that, in that two cases, the effect of wall adhesion on the oil phase became significant.

3.3. Calculated velocity field

Fig. 5 compares the predicted values of the axial mean velocity and the experiment data given by Elseth et al. [13]. The agreement is quite reasonable. It is notable that

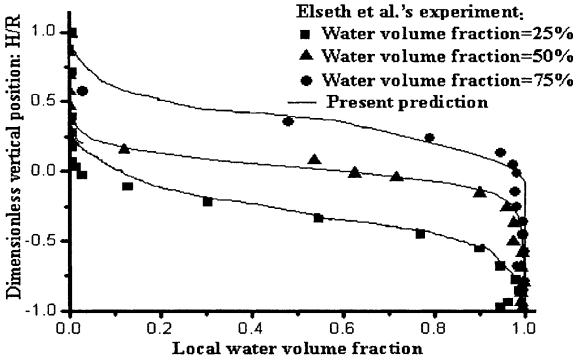

Fig. 4. Comparison between predicted and experimental value of local phase fraction.

the model can predict the position of peak velocity. The effect of interface to the velocity field is successfully simulated. However, the calculated water velocities exceed the experimental data by 12% at the water volume fraction of 25% and the calculated oil velocities is slightly over-predicted when the water volume fraction is 75%.

Extensive calculations were carried out at the mixed velocities of 0.5, 1.0, 1.5, 2.0 m/s, respectively. From numerical results, the velocity field is strongly affected by the water volume fraction and interface. When the water volume fraction is less that 50%, the highest axial velocity is positioned the oil phase. The position of highest axial velocity transfers to the water phase when the input water fraction became up to 65%. And there is a slightly decrease of axial velocity in region between the two phases.

3.4. Correlation for pressure drop

The empirical parameters X and ϕ are used to represent pressure drop data of stratified water–oil flows, with X and ϕ defined as

$$X^2 = \frac{\frac{0.184}{d}\left(\frac{u_{sw}d}{v_w}\right)^{0.2}\frac{\rho_w u_{sw}^2}{2}}{\frac{0.184}{d}\left(\frac{u_{so}d}{v_o}\right)^{0.2}\frac{\rho_o u_{so}^2}{2}}, \quad \Phi = \frac{u_{so}}{u_{sw}} \tag{19}$$

where u_{so}, u_{sw} are superficial velocity of oil phase and water phase, respectively. Based on the numerical results, the correlation for pressure drop is represented by

$$(\mathrm{d}p/\mathrm{d}z)_{TP} = \phi^{-1.87}X^{-2.02}\left(\frac{\mathrm{d}p}{\mathrm{d}z}\right)_m \tag{20}$$

where $(\mathrm{d}p/\mathrm{d}z)_{TP}$ is the stratified water–oil flow pressure drop, $(\mathrm{d}p/\mathrm{d}z)_m$ is calculated by

$$(\mathrm{d}p/\mathrm{d}z)_m = \frac{f_m}{d}\frac{\rho_m u_m^2}{2} \tag{21}$$

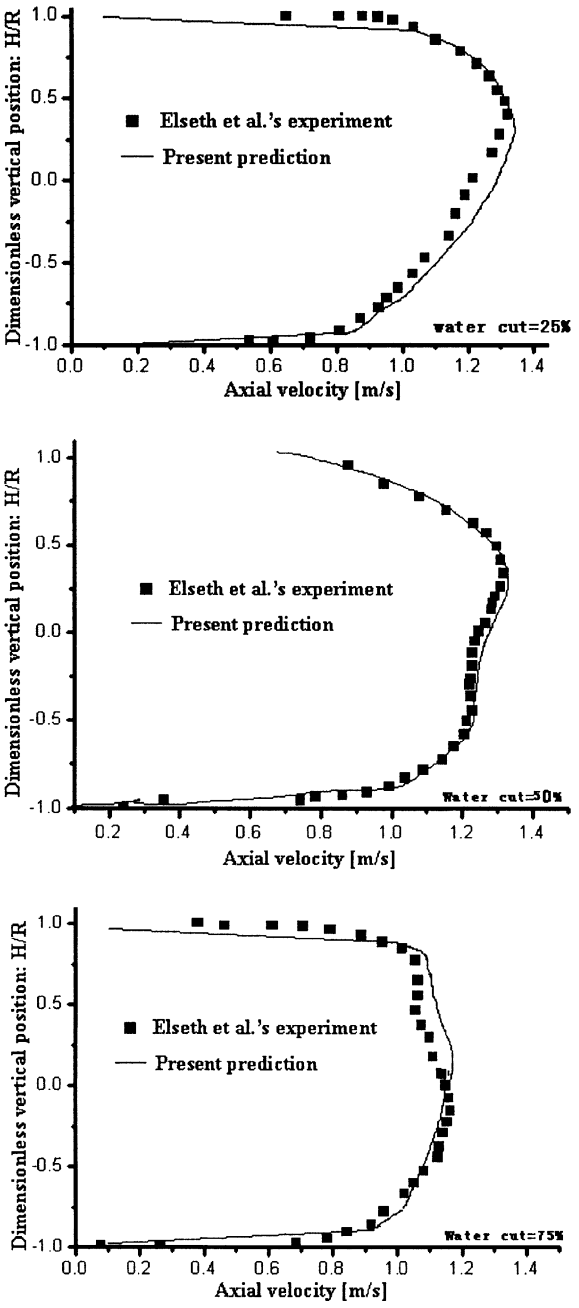

Fig. 5. Comparison of predicted and experimental mean axial velocity.

with $f_m = 0.3164/Re_m^{0.25}$, $Re_m = \rho_m u_m d/\mu_m$, $u_m = u_{so} + u_{sw}$, $\rho_m = \beta_o\rho_o + (1-\beta_o)\rho_w$, $\mu_m = \beta_o\mu_o + (1-\beta_o)\mu_w$.

3.5. Correlation for oil holdup

By analyzed the numerical results, the correlation for mean oil holdup can be represented as

$$\alpha_o = \frac{1.3124\beta_o}{1 + 0.3124\beta_o} \tag{22}$$

where β_o is volume fraction of oil phase.

4. Conclusions

Stratified oil–water two-phase turbulent flow in a horizontal tube is numerically simulated using a VOF model. Predictions of pressure loss and slip ratio showed acceptable agreement with experimental data [13]. The predicted local phase fraction profile agrees with experimental results very well. The prediction of velocity field is quite satisfactory. Extensive calculations are carried out for the cases of various phase fractions and flowrates. Based on the numerical results, flow field characteristics are described and correlations for pressure loss and mean liquid holdups are presented.

Although the present formulation is rather complex and demands much computational time, due to the nature of the turbulent model and the fine grids required for its implementation, it does appear to demonstrate that the CFD technique can be successfully applied to stratified turbulent liquid–liquid flows.

Acknowledgements

The financial supports for this study by the National Natural Science Foundation of China (59995462) and (10172069) are gratefully acknowledged.

References

[1] P.B. Baxendall, R. Thomas, The calculation of pressure gradients in high-rate flowing wells, J. Pet. Technol. 13 (10) (1961) 1023–1028.
[2] H.D. Beggs, J.P. Brill, A study of two-phase flow in inclined pipes, J. Pet. Technol. 25 (5) (1973) 607–617.
[3] J.M. Mandhane, G.A. Gregory, K. Aziz, Critical evaluation of friction pressure-drop prediction methods for gas–liquid flow in horizontal pipes, J. Pet. Technol. 29 (11) (1977) 1348–1358.
[4] V. Battara, O. Mariani, M. Gentilini, G. Giachetta, Condensate line correlations for calculating holdup, friction compared to field data, Oil Gas J. 83 (12) (1985) 148–152.
[5] G.A. Gregory, M. Fogarasi, A critical evaluation of multiphase gas–liquid pipelines calculation methods, in: Proceedings of the second international conference on multiphase flow, London, 1985, pp. 93–108.
[6] Y. Taitel, A.E. Dukler, A model for predicting flow regime transitions in horizontal and near horizontal Gas–liquid flow, AIChE J. 22 (1) (1976) 47–55.
[7] J. Hart, P.J. Hamersma, J.M.H. Fortuin, Correlations predicting frictional pressure drop and liquid holdup during horizontal gas liquid pipe flow with a small liquid holdup, Int. J. Multiphase Flow 15 (5) (1989) 947–964.
[8] X.T. Chen, X.D. Cai, J.P. Brill, Gas–liquid stratified-wavy flow in horizontal pipelines, J. Energy Res. Technol. 119 (2) (1997) 209–216.
[9] N.A. Vlachos, S.A. Paras, A.J. Karabelas, Prediction of holdup, axial pressure gradient and wall shear stress in wavy stratified and stratified/atomisation gas/liquid flow, Int. J. Multiphase Flow 25 (3) (1999) 365–376.
[10] O. Shoham, Y. Taitel, Stratified turbulent–turbulent gas–liquid flow in horizontal and inclined pipes, AIChE J. 30 (2) (1984) 377–385.
[11] R.I. Issa, Prediction of turbulent, stratified, two-phase flow in inclined pipes and channels, Int. J. Multiphase Flow 14 (1) (1988) 141–154.
[12] C.H. Newton, M. Behnia, Numerical calculation of turbulent stratified gas–liquid pipe flows, Int. J. Multiphase Flow 24 (5) (1998) 327–337.
[13] G. Elseth, H.K. Kvandal, M.C. Melaaen, Measurement of velocity and phase fraction in stratified oil/water flow, International Symposium on Multiphase Flow and Transport Phenomena, Antalya, Turkey, 2000, pp. 206–210.
[14] J.U. Brackbill, D.B. Kothe, C. Zemach, A continuum method for modeling surface tension, J. Comp. Phys. 100 (1992) 335–354.
[15] W.P. Jones, B.E. Launder, The prediction of laminarization with a two-equation model of turbulence, Int. J. Heat Mass Transfer 15 (4) (1972) 301–311.
[16] C.K.Y. Lam, K. Bremhost, A modified form of the k–ε model for prediction wall temperature, ASME. J. Fluids Eng. 103 (2) (1981) 456–460.